Statistical Analysis of Progressive Interval Type-I Partially Accelerated Test and Its Inspection of Optimum Periods

Refah Alotaibi[1], Chanseok Park[2], Hoda Rezk[3,*] and Ahmed Elshahhat[4]

[1] Department of Mathematical Sciences, College of Science, Princess Nourah bint Abdulrahman University, Riyadh, 11671, Saudi Arabia

[2] Applied Statistics Laboratory, Department of Industrial Engineering, Pusan National University, Busan, 46241, Republic of Korea

[3] Department of Statistics, Al-Azhar University, Cairo, 11884, Egypt

[4] Faculty of Technology and Development, Zagazig University, Zagazig, 44519, Egypt

INFORMATION

Keywords:
Partially accelerated test
optimum inspection period
censoring
likelihood
length-biased-exponential
Monte Carlo experiments
physics data modeling

DOI: 10.23967/j.rimni.2025.10.65809

Revista Internacional de Métodos Numéricos para Cálculo y Diseño en Ingeniería

Statistical Analysis of Progressive Interval Type-I Partially Accelerated Test and Its Inspection of Optimum Periods

Refah Alotaibi[1], **Chanseok Park**[2], **Hoda Rezk**[3,*] **and Ahmed Elshahhat**[4]

[1]Department of Mathematical Sciences, College of Science, Princess Nourah bint Abdulrahman University, Riyadh, 11671, Saudi Arabia

[2]Applied Statistics Laboratory, Department of Industrial Engineering, Pusan National University, Busan, 46241, Republic of Korea

[3]Department of Statistics, Al-Azhar University, Cairo, 11884, Egypt

[4]Faculty of Technology and Development, Zagazig University, Zagazig, 44519, Egypt

ABSTRACT

This study explores a general framework for reliability analysis named progressive interval Type-I censoring within a multi-stage step-stress partially accelerated life testing setting. A more flexible alternative to the traditional exponential model, known as the length-biased exponential (LBE) distribution, is employed to model failure times. Due to its symmetrical feature, it has extensive applications in real-world domains such as survival analysis, actuarial science, reliability, and mathematical finance. The maximum likelihood approach of estimation is utilized to estimate the model parameters, along with bootstrapping techniques to assess estimation efficiency. Confidence intervals for the LBE parameters are also derived based on asymptotic variances. To optimize the inspection period, two competing optimality criteria—variance minimization (Var-optimality) and determinant maximization (D-optimality)—are investigated. A comprehensive Monte Carlo simulation study is conducted to evaluate the performance of different estimation strategies, demonstrating the superiority of the proposed methodology. Steel is particularly valued for its toughness, wear resistance, and hardness, all of which can be significantly modified through heat treatment and annealing processes. So, a real-world application using hardened steel failure data validates the practical relevance of the developed inferential framework. The findings offer valuable insights for statisticians and reliability engineers in designing efficient life-testing experiments under constrained resources.

OPEN ACCESS

Received: 21/03/2025

Accepted: 07/05/2025

Published: 22/09/2025

DOI
10.23967/j.rimni.2025.10.65809

Keywords:
Partially accelerated test
optimum inspection period
censoring
likelihood
length-biased-exponential
Monte Carlo experiments
physics data modeling

1 Introduction

One frequently works with high-quality, incredibly dependable devices with a sizable lifespan due to ongoing advancements in manufacturing design. It's more challenging to find out the lifespan of highly reliable equipment during testing under typical circumstances. Because of this, lifetime testing

*Correspondence: Hoda Rezk (hodaragab2009@yahoo.com).

under typical circumstances is very expensive and time-consuming. To get failures in a short amount of time, the most popular methods are the partially accelerated life test (P-ALT) and the accelerated life test (ALT), where test units are performed under higher-than-usual stress conditions. To cause early failures, units are tested under high-stress conditions. The failure data is then correlated with the operational stress level using a specified stress-dependent model.

The P-ALT is appropriate in place of the ALT when the model in question is unknown. The units in ALTs are only operated under accelerated circumstances or stress. They are, nevertheless, operated at both accelerated and use conditions in P-ALTs. As a result, an experiment item is first run at a usage condition using step-stress P-ALTs, and if it keeps working well after a while, it is then run at an accelerated condition until it breaks or the observation is censored; refer to Ismail [1]. Then, the P-ALT integrates both standard and accelerated life testing. P-ALTs aim to gather more failure data in a shorter amount of time without subjecting all test units to high stresses. As indicated by Nelson [2], the stress loading in a P-ALT can be applied by several methods. They include constant-stress, step-stress, and progressive-stress. Every unit in constant-stress testing is run at a constant stress level until the test is finished, with P-ALTs running each item at either the usage condition or the accelerated condition only.

On the other hand, a test unit experiences progressively greater stress levels during the step-stress P-ALTs. A test unit operates for a predetermined amount of time at a predetermined low stress. Stress on it is increased and maintained for a predetermined time if it fails. Consequently, tension builds up gradually until the test equipment malfunctions. Test units typically follow a predetermined pattern of stress levels and test durations. We refer to the most basic step-stress P-ALT as simple step-stress P-ALT because it simply employs two stress levels. Many scholars have examined the statistical conclusions in this step-stress P-ALT, including Tang et al. [3], Xiong [4], Gouno et al. [5], Abdel-Hamid and Al-Hussaini [6], Ismail and Aly [7], and more recently Pushkarna et al. [8], EL-Sagheer and Hasaballah [9], Alotaibi et al. [10], Prakash et al. [11], Maurya et al. [12], among others.

The goal of these studies is to gather more failure data in a shorter amount of time without subjecting every test unit to extreme stress. Step-stress P-ALTs are useful for many life-testing issues where the test procedure takes a while if the test is only conducted under use conditions, as Rahman et al. [13] pointed out. Step-stress P-ALTs are generally simpler to use and offer several benefits, such as time savings, cost-effectiveness, and flexibility. Usually, ALTs or P-ALTs are used under censored sampling to save additional time and cost. Type-I and Type-II censoring plans are the most widely used techniques. Aside from the ultimate termination point, they do not let units be taken out of the test. These factors bring us to the topic of progressive censoring, which allows for the effective use of the resources at hand by removing a certain amount of test units that have not failed after each testing phase. The current work tries to integrate P-ALTs via a progressive mechanism before focusing on the best possible selection of stress level change points. Additionally, it investigates the selection of the inspection interval's duration based on length-biased exponential (LBE) distribution sample findings. We examine the process of choosing between two contradictory optimality criteria: Var- and D-optimality; for more details, see Gouno et al. [5] and Newer et al. [14].

The main contribution of this paper is fivefold:

- First, we analyze the LBE model from progressive interval Type-I censoring (PIC-T1) with equal inspection intervals for the multiple-stage step-stress partially accelerated life test.
- Second, we discuss the estimation of the model parameter under the frequentist approach via the method of maximum likelihood, and we determine the associated measures.

- Third, we construct the bounds associated with the asymptotic confidence interval by utilizing the information estimated from the observed Fisher information.
- Fourth, we also invoke the idea of bootstrapping re-sampling techniques via the bootstrap-p approach to examine the efficiency of the estimations of the unknown LBE parameters in such a scenario.
- Fifth, we provide the optimal lengths of inspection intervals in the proposed strategy when dealing with the LBE distribution.
- Lastly, we performed an extensive simulation examination and a real-world physical example to analyze the performance of different estimations, and several recommendations were drawn. Applied practitioners, statisticians, and reliability engineers working in this subject should find significant interest in the framework that this paper lays out as a guide for choosing the optimum estimating method among the various inferential methods.

The rest of the paper is classified as follows: Section 2 provides the model description. Section 3 investigates the maximum likelihood method. Interval estimations are provided in Section 4. Criteria for optimal interval length are examined in Section 5. Monte Carlo results are reported in Section 6. In Section 7, a real application based on hardened steel specimen data is explored. Lastly, Section 8 provides some concluding remarks and recommendations for the study.

2 Model Description and Censoring Plan

The multiple-stage (or k-stage) step-stress P-ALT with PIC-T1 will be discussed as follows: The life-testing experiment, which uses progressively Type-I interval censored data, involves placing n units in a k-level P-ALT. Up until time τ, the units are operated at stress level S_1. During this period, the number of failed units (n_1) and the number of removed units (m_1) are noted. More stress S_2 is now applied to the remaining $(n - n_1 - m_1)$ survival units beginning at time τ, and they continue until time 2τ, at which point the number n_2 of failed units and the number m_2 of removed units within the interval $(\tau, 2\tau]$ are recorded, and so forth. The following constraints describe the model assumptions:

1. There are successively k-level of higher stresses $S_1 < S_2 < \ldots < S_k$ and $k - 1$ predetermined inspection times: $\tau < 2\tau < \ldots < (k-1)\tau < k\tau = \infty$, where the normal used stress is assumed to be $S_1 = 0$.
2. The point $(k - 1)\tau$ at which the remaining tested units fail or are eliminated from the test is known as the termination test time. This suggests that the following are the intervals of inspection: $(0, \tau], (\tau, 2\tau], \ldots, ((k - 1)\tau, \infty)$.
3. The probabilities of the removed units m_j, π_j, $j = 1, 2, \ldots, k - 1$ are randomly determined by the experimenter.
4. According to the LBE indexed by the scale parameter σ_j, which has the inverse power function provided by $\sigma_j = cS_j^{-p}$ at the level stress S_j, $j = 1, 2, \ldots, k$, the lifetimes of the n tested units are distributed uniformly. When the power of the applied stress is denoted by the parameter $p > 0$ and the constant of proportionality by the parameter c.

Extended versions of popular distributions, like the LBE distribution, are recognized to offer more modeling flexibility in various fields, including actuarial, medical, economic, financial, demographic, and lifetime analytic sciences. The LBE model is, therefore, determined to be more flexible than the exponential distribution. As mentioned in Dara and Ahmad [15], the exponential distribution weight in line with Fisher's idea can be used to create the LBE distribution. They also stated that its hazard rate function is more flexible than the traditional exponential model. However, the probability density function (PDF), cumulative distribution function (CDF), and hazard rate function (HRF) of the LBE (ξ) distribution are provided by

$$f(x;\xi) = \frac{x}{\xi^2} e^{-\frac{x}{\xi}}, \tag{1}$$

$$F(x;\xi) = 1 - \left(1 + \frac{x}{\xi}\right) e^{-\frac{x}{\xi}}, \tag{2}$$

and

$$h(x;\xi) = \frac{x}{\xi^2} \left(1 + \frac{x}{\xi}\right)^{-1}, \tag{3}$$

respectively, where $\xi > 0$ is the scale parameter and $x > 0$. Note that the reliability (or survival) function (RF) is obtained by $R(\cdot) = 1 - F(\cdot)$. Utilizing various selections of ξ, Fig. 1 depicts several shapes for the density and failure rates of the LBE model. It is noticeable that the LBE density can be used to model data that are mostly positively skewed. It also evidences the LBE failure rate that can be analyzed with increasing HRFs, which is frequently used in reliability examinations.

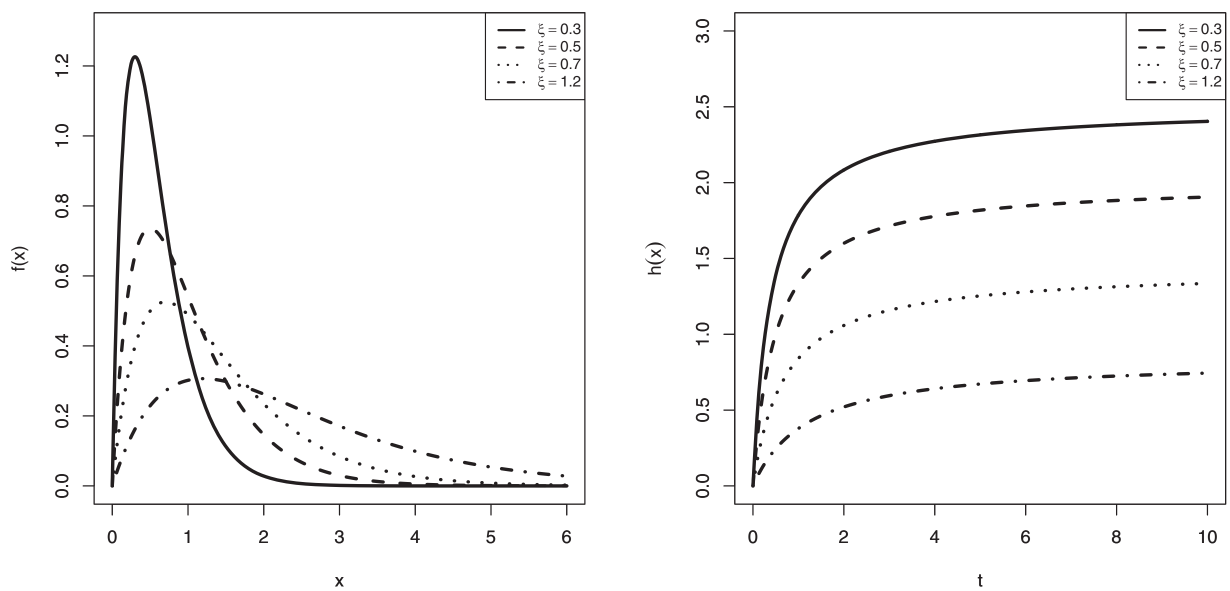

Figure 1: Several shapes of the PDF (left) and HRF (right) of the LBE distribution

Let us now examine the k-stage step-stress P-ALT with equal inspection intervals of length τ under PIC-T1. Consequently, the CDF is provided by the cumulative exposure model's assumptions, which

$$F(x) = \begin{cases} 1 - \left(1 + \frac{x}{\xi}\right) e^{-\frac{x}{\xi}}, & \text{if } 0 < x \leq \tau, \\ 1 - \left(1 + \frac{1}{\xi}\left(\tau + \delta_1(x-\tau)\right)\right) e^{-\frac{\left(\tau + \delta_1(x-\tau)\right)}{\xi}}, & \text{if } \tau < x \leq 2\tau, \\ \vdots \\ 1 - \left(1 + \frac{1}{\xi}\left((k-1)\tau + \delta_{k-1}\left(x-(k-1)\tau\right)\right)\right) e^{-\frac{\left((k-1)\tau + \delta_{k-1}(x-(k-1)\tau)\right)}{\xi}}, & \text{if } (k-1)\tau < x \leq \infty. \end{cases} \tag{4}$$

Thus, the test unit's PDF is provided by

$$f(x) = \begin{cases} \frac{x}{\xi^2} e^{-\frac{x}{\xi}}, & \text{if } 0 < x \leq \tau, \\ \frac{(\tau + \delta_1(x-\tau))}{\xi^2} e^{-\frac{\left(\tau + \delta_1(x-\tau)\right)}{\xi}}, & \text{if } \tau < x \leq 2\tau, \\ \vdots \\ \frac{((k-1)\tau + \delta_{k-1}\left(x-(k-1)\tau\right))}{\xi^2} e^{-\frac{\left((k-1)\tau + \delta_{k-1}(x-(k-1)\tau)\right)}{\xi}}, & \text{if } (k-1)\tau < x \leq \infty. \end{cases} \tag{5}$$

3 Likelihood Inference

In statistics, one of the most significant and often applied techniques is the maximum likelihood. The goal of maximum likelihood parameter estimation is to identify the parameters that will maximize the sample data's probability or likelihood. Moreover, maximum likelihood estimators (MLEs) are flexible and can be used with a wide range of models and data kinds. Furthermore, they offer effective techniques for measuring uncertainty using confidence bounds. These estimators are computed numerically because they are not always available in closed form. This section presents the maximum likelihood method-based point and interval estimates of the model parameters and acceleration factor based on the gradually PIC-T1 data. Additionally, the model parameters and acceleration factor's Fisher information matrix (FIM) are shown.

Assume that $n_1, n_2, \ldots, n_k$ is a sample from a k-stage step-stress P-ALT that has been gradually PIC-T1 using the censoring scheme $m = (m_1, m_2, \ldots, m_k)$. That is, while testing in the interval $((i-1)\tau, i\tau]$ at stress x_i, where $i = 1, 2, \ldots, k$, the number of failed units, n_i, is noted. Thus, we obtain that $n_i | n_{i-1}, \ldots, n_1 \sim binomial(b_i, F_i(\tau))$, where $b_i = n - \sum_{j=1}^{i-1} n_j - \sum_{j=1}^{i-1} m_j$ and $F_i(\tau) = \frac{F(i\tau) - F\left((i-1)\tau\right)}{1 - F\left((i-1)\tau\right)}$.

The likelihood function is provided by

$$L \propto \prod_{i=1}^{k} \left[F(i\tau) - F\left((i-1)\tau\right)\right]^{n_i} \left[1 - F(i\tau)\right]^{m_i}. \tag{6}$$

The likelihood function's natural logarithm, $\mathcal{L} = \ln L$, can be expressed as

$$\mathcal{L} = \sum_{i=1}^{k} \left\{ n_i \ln \left[\omega_{(i-1)} - \omega_i \right] - m_i \ln \left[\omega_i \right] \right\}, \tag{7}$$

where

$$\omega_i = \left(1 + \frac{1}{\xi} \left(i\tau + \delta_i (x - i\tau)\right)\right) e^{-\frac{\left(i\tau + \delta_i (x - i\tau)\right)}{\xi}}$$

and

$$\omega_{(i-1)} = \left(1 + \frac{1}{\xi} \left((i-1)\tau + \delta_{(i-1)} \left(x - (i-1)\tau\right)\right)\right) e^{-\frac{\left((i-1)\tau + \delta_{(i-1)} (x - (i-1)\tau)\right)}{\xi}}.$$

Upon computing the initial partial derivatives of (7) concerning ξ and δ_i, we obtain the likelihood equations as follows:

$$\begin{aligned}\frac{\partial \mathcal{L}}{\partial \xi} = &\sum_{i=1}^{k} n_i (\omega_{(i-1)} - \omega_i)^{-1} \left[e^{-\frac{\gamma_{(i-1)}(x)}{\xi}} \left(\gamma_{(i-1)}(x) + \xi^{-3} \gamma_{(i-1)}^2(x)\right) - e^{-\frac{\gamma_i(x)}{\xi}} \left(\gamma_i(x) + \xi^{-3} \gamma_i^2(x)\right) \right] \\ &- m_i \omega_i^{-1} \left(\left(\frac{-1}{\xi^2} \left(\gamma_i(x)\right) \right) e^{-\frac{\gamma_i(x)}{\xi}} + \left(1 + \frac{1}{\xi} \left(\gamma_i(x)\right)\right) \left(\frac{\gamma_i(x)}{\xi^2} \right) e^{-\frac{\left(\gamma_i(x)\right)}{\xi}} \right),\end{aligned} \tag{8}$$

and

$$\begin{aligned}\frac{\partial \mathcal{L}}{\partial \delta_i} = &\sum_{i=1}^{k} n_i (\omega_{(i-1)} - \omega_i)^{-1} \\ &\times \left[\left(\frac{x - (i-1)\tau}{\xi^2} \right) e^{-\frac{\gamma_{(i-1)}(x)}{\xi}} \left(\gamma_{(i-1)}(x) + \gamma_{(i-1)}^2(x)\right) - \left(\frac{x - i\tau}{\xi^2} \right) e^{-\frac{\gamma_i(x)}{\xi}} \left(\gamma_i(x) + \gamma_i^2(x)\right) \right] \\ &- m_i \omega_i^{-1} \left((x - i\tau) e^{-\frac{\gamma_i(x)}{\xi}} - \left(1 + \frac{1}{\xi} \left(\gamma_i(x)\right)\right) \frac{(x - i\tau)}{\xi} e^{-\frac{\left(\gamma_i(x)\right)}{\xi}} \right),\end{aligned} \tag{9}$$

where $\gamma_{(i-1)}(x) = \left((i-1)\tau + \delta_{(i-1)} \left(x - (i-1)\tau\right)\right)$ and $\gamma_i(x) = (i\tau + \delta_i(x - i\tau))$.

We now have a system of two non-linear likelihood equations in two unknowns, ξ and δ_i, (8) and (9). It is impossible to resolve analytically. The estimations are obtained by the Newton-Raphson (N-R) iteration approach.

4 Interval Inference

This section deals with obtaining the confidence intervals (CIs) of the unknown subjects. Since our point estimate is the most likely value(s) for the parameter, it should serve as the foundation for the confidence intervals. A set of values called CIs is used to provide precise estimations for an unknown population characteristic. In this experiment, two different types of CIs were estimated.

4.1 Asymptotic Intervals

Normality-based asymptotic CIs (ACIs) are not very effective because Eq. (1)'s density is not symmetric. The population under investigation is thought to adhere to the probability distribution found in Eq. (1). Using a normal approximation or standardization in conjunction with the bootstrapping interval is possible. When the exact distribution of a statistic is known, the resulting confidence interval is exact and provides a coverage probability equal to the stated confidence level (e.g., 95%). In contrast, ACIs only approximate the confidence level—often under-performing for small samples—but their accuracy improves with larger sample sizes, and methods like Wilson intervals or techniques such as studentization process, Z transformation, and maximum likelihood estimation can enhance their reliability. For additional details, one may refer to Deshmukh and Kulkarni [16]. Assuming that $\vartheta = (\xi, \delta_i)$. It has been established that the asymptotic distribution of MLE values of $N(0,\rho)$ is produced by $[(\widehat{\xi} - \xi),\ (\widehat{\delta_i} - \delta_i)]$ where $\rho = \rho_{ij},\ i,j = 1,2$. The inverse of the FIM, which is provided subsequently, is an estimate of the asymptomatic variance-covariance matrix, as was previously mentioned. The approximately $100(1-\varnothing)\%$ two-sided CIs for $\varnothing$ are provided by

$$\left(\widehat{\vartheta}_{il},\ \widehat{\vartheta}_{iu}\right):\ \widehat{\vartheta}_i \mp z_{1-\frac{\varnothing}{2}}\sqrt{\widehat{\rho_{ij}}},\ i = 1,2,$$

where $z_{1-\frac{\varnothing}{2}}$ represents the standard normal distribution's $100\left(1-\frac{\varnothing}{2}\right)$th upper percentile.

This subsection formulates the FIM for $\vartheta = (\xi,\ \delta_i)$ as

$$I_{2\times 2}(\vartheta) = -E\begin{bmatrix} \in_{11} & \in_{12} \\ \in_{21} & \in_{22} \end{bmatrix}, \tag{10}$$

where $\in_{11} = \frac{\partial^2 \mathcal{L}}{\partial \xi^2}$, $\in_{12} = \in_{21} = \frac{\partial^2 \mathcal{L}}{\partial \xi \partial \delta_i}$, and $\in_{22} = \frac{\partial^2 \mathcal{L}}{\partial \delta_i^2}$, such as

$$\begin{aligned}
\frac{\partial^2 \mathcal{L}}{\partial \xi^2} &= \sum\nolimits_{i=1}^{k} \frac{n_i}{\left(\omega_{(i-1)} - \omega_i\right)^2} \\
&\times \Bigg\{ \Bigg(e^{-\frac{\gamma_{(i-1)}(x)}{\xi}} \gamma_{(i-1)}^2(x) \Big\{ \left(\xi^{-3}\left(1 - 3\xi^{-1}\right) - 1\right) - e^{-\frac{\gamma_{(i-1)}(x)}{\xi}} \left(\gamma_{(i-1)}(x) + \xi^{-3}\gamma_{(i-1)}^2(x)\right) \Big\} \left(\omega_{(i-1)} - \omega_i\right) \Bigg) \\
&- \left(e^{-\frac{\gamma_i(x)}{\xi}} \gamma_i^2(x) \Big\{ \left(\xi^{-3}\left(1 - 3\xi^{-1}\right) - 1\right) - e^{-\frac{\gamma_i(x)}{\xi}} \left(\gamma_i(x) + \xi^{-3}\gamma_i^2(x)\right) \Big\} \right)^2 \Bigg\}, \\
\frac{\partial^2 \mathcal{L}}{\partial \delta_i^2} &= \sum\nolimits_{i=1}^{k} \Bigg\{ \frac{n_i}{\left(\omega_{(i-1)} - \omega_i\right)^2} \\
&\times \Bigg\{ \left(\omega_{(i-1)} - \omega_i\right) \left(\frac{(x-(i-1)\tau)^2}{\xi^2} \right) e^{-\frac{\gamma_{(i-1)}(x)}{\xi}} \left(1 + 3\gamma_{(i-1)}(x) + \gamma_{(i-1)}^2(x)\right) \\
&- \left(\frac{(x - i\tau)^2}{\xi^2} \right) e^{-\frac{\gamma_i(x)}{\xi}} \left(1 + 3\gamma_i(x) + \gamma_i^2(x)\right) - \Bigg[\Bigg(\left(\frac{x-(i-1)\tau}{\xi^2} \right) e^{-\frac{\gamma_{(i-1)}(x)}{\xi}} \left(\gamma_{(i-1)}(x) + \gamma_{(i-1)}^2(x)\right) \\
&- \left(\frac{x - i\tau}{\xi^2} \right) e^{-\frac{\gamma_i(x)}{\xi}} \left(\gamma_i(x) + \gamma_i^2(x)\right) \Bigg) \left(\frac{(i\tau - (i-1)\tau)}{\xi} \right) \Bigg] \Bigg\} \Bigg\},
\end{aligned}$$

and

$$\frac{\partial^2 \mathcal{L}}{\partial \xi \partial \delta_i} = \sum_{i=1}^{k} \frac{n_i}{\left(\omega_{(i-1)} - \omega_i\right)^2}$$

$$\times \left\{ \left(\omega_{(i-1)} - \omega_i\right) \left\{ e^{-\frac{\gamma_{(i-1)}(x)}{\xi}} \left[\left(x - (i-1)\tau\right) \left(1 + \gamma_{(i-1)}(x) + 2\xi^{-3}\gamma_{(i-1)}(x) + \gamma_{(i-1)}^2(x)\right) \right] \right. \right.$$

$$+ e^{-\frac{\gamma_i(x)}{\xi}} \left[\left(x - i\tau\right) \left(1 + \gamma_i(x) + 2\xi^{-3}\gamma_i(x) + \gamma_i^2(x)\right) \right] \Big\} - \left(e^{-\frac{\gamma_{(i-1)}(x)}{\xi}} \left(\gamma_{(i-1)}(x) + \xi^{-3}\gamma_{(i-1)}^2(x)\right) \right.$$

$$\left. \left. - e^{-\frac{\gamma_i(x)}{\xi}} \left(\gamma_i(x) + \xi^{-3}\gamma_i^2(x)\right) \right) \left(\frac{i\tau - (i-1)\tau}{\xi} \right) \right\}.$$

Notably, the observed FIM can be acquired, although the expectation of the values derived from the log-likelihood second derivatives of the parameters is nearly impossible to obtain. While traditional techniques for getting interval estimates frequently fail to produce sufficient results, a popular alternative known as the resampling (alias Bootstrap) technique has gained widespread popularity. Next, we'll look at creating confidence intervals using the bootstrapping technique.

4.2 Bootstrapping Intervals

We recommend applying the percentile bootstrap technique (Boot-p), which is a popular member of the bootstrap techniques. When the underlying distribution is an LBE distribution, there are situations when the standard error of the point estimator is unknown. These scenarios frequently entail complex variations and difficult applications of the standard expectation and variance operators. As a workaround, one computationally intensive method that can be used to address this problem is bootstrapping. Here are brief illustrations of both approaches, together with detailed directions; for more details, see Chernick and LaBudde [17]. To conduct the Boot-p method, do the following steps:

Step-1: Calculate $\widehat{\xi}$ and $\widehat{\delta}_i,\ i = 1, 2, \ldots, k$, from a PIC-T1 sample.

Step-2: For each i within 1 and k, use the results in Step-1 to create a bootstrap sample from the LBE distribution.

Step-3: Obtain $\widehat{\xi}^*$ and $\widehat{\delta}_i^*$ of $\widehat{\xi}$ and $\widehat{\delta}_i$ for $i = 1, 2, \ldots, k$.

Step-4: Redo Steps 2–3 $\mathcal{B}$ times, then order $\widehat{\xi}^*$ and $\widehat{\delta}_i^*$ to get the bootstrap sample as

$\left(\widehat{\vartheta}_w^{*[1]}, \widehat{\vartheta}_w^{*[2]}, \ldots, \widehat{\vartheta}_w^{*[\mathcal{B}]}\right)$,

where $w = 1, 2$, $\widehat{\vartheta}_1^* = \widehat{\xi}^*$ and $\widehat{\vartheta}_2^* = \widehat{\delta}_i^*,\ i = 1, 2, \ldots, k$.

Step-5: Let $\Phi(x) = P\left(\widehat{\vartheta}_w^* \le x\right)$ is the CDF for a given x. Define $\widehat{\vartheta}_{wBoot-p}^* = \Phi^{-1}(x)$. The estimated $100(1-\varnothing)\%$ percent confidence interval of ϑ may be found as

$$\left(\widehat{\vartheta}_{wBoot-p}^* \left(\frac{\varnothing}{2}\right), \widehat{\vartheta}_{wBoot-p}^* \left(1 - \frac{\varnothing}{2}\right)\right).$$

5 Optimum Inspection Length

Examining the selection of τ, the inspection interval length, in k-stage step-stress PALT with PIC-T1 is one of the paper's objectives. We present two selection criteria in this section that allow one to determine the ideal value of τ.

5.1 Var-Optimality

In a reliability investigation, the mean lifespan is a crucial component. In a step-stress environment, the researcher is often interested in obtaining the most accurate mean life estimate at design (use) stress. At the design (use) stress, from (5), the mean lifetime (denoted by US_0) is given by 2ξ.

Let the MLE, $\widehat{US}_0$, denote the mean lifetime at the design (use) stress US_0. The criterion function is defined as the asymptotic variance (AVar) of $\ln(\widehat{US}_0)$ MLE as

$$\tau_V^\star = AVar\left[\ln\left(\widehat{US}_0\right)\right]$$
$$= n\left(\xi^\circ, X_0\right) I^{-1}\left(\xi, \delta_i\right)\left(\xi^\circ, X_0\right)^\top,$$

where X_0 represents the stress under use and ξ° is the first derivative of ξ. Next, by minimizing $\tau_V^\star$, the variance optimal τ is found.

5.2 D-Optimality

Fisher's information matrix determinant serves as the foundation for the second optimal criterion. It has been widely applied to the process of organizing life tests. Determinant optimality, which takes into account the entire parameter space, is a more reasonable criterion if one is more interested in highly precise estimation. The generalized asymptotic variance (GAV) of the model parameter MLEs can be used to construct it. It is known that the GAV is proportional to the reciprocal of the determinant of the Fisher information matrix; hence, maximizing this determinant is equivalent to decreasing the GAV. For more details, read Bai et al. [18]. The criterion function (denoted by $\tau_D^\star$) is then defined by

$$\tau_D^\star = \frac{1}{\left|I(\hat{\xi}, \hat{\delta}_i)\right|},\ i = 1, 2, \ldots, k.$$

As a result, the ideal inspection interval duration is selected, minimizing GAV. It is observed that Fisher's information matrix serves as the foundation for both the Var-optimality and D-optimality criteria. These standards have been widely applied in the process of choosing designs for planned experiments. Practically, when a dataset of PIC-T1 using a k-stage step-stress P-ALT is available, the smallest value of the Var-optimality criterion and the highest value of the D-optimality criterion will produce the best inspection interval duration.

6 Monte Carlo Comparisons

To assess and compare the real behavior of the acquired point and interval estimators of the LBE lifetime model, we generate 1000 random samples from PIC-T1 using a k-stage step-stress P-ALT with equal inspection intervals. For this objective, without loss of generality, we set $k = 4$, $\xi = 0.5$, and $(n = 30, 60, 100, 150, 200)$. Taking $(\tau_1,\ \tau_2,\ \tau_3,\ \tau_4) = (0.5,\ 1.0,\ 1.5,\ 2.0)$, different scenarios with respect to the stress levels $(\delta_1, \delta_2, \delta_3, \delta_4)$, namely (0.5, 1.0, 1.5, 2.0) and (0.75, 1.25, 1.75, 2.25) are also considered. Here, we assumed that the lengths of all inspection periods are similar for simplicity.

Making use of the `maxLik` programming package in R (version 4.2.2), we calculate all acquired point and interval estimators of ξ and δ_i. Additionally, we recommend using the **maxNR** optimization function to apply the N-R method, which is available in the **maxLik** package. The initial guess points used to run the N-R iterative sampler are taken as the actual values of ξ and δ_i proposed in this part.

With a constraint $\pi_k = 1$, three proportion styles of π_i for $i = 1, 2, 3$, of the progressive-censoring (PC) for m_i for $i = 1, 2, \ldots, 4$, are utilized in the simulation processes, namely PC [1] $= \pi_i = 0.05$, PC [2] $= \pi_i = 0.15$, and PC [3] $= \pi_i = 0.25$ for $i = 1, 2, 3$.

In all calculation settings, the average estimates (Av.Es) of ξ (as an example) are given by

$$\text{Av.E}(\breve{\xi}) = \frac{1}{1000}\sum_{\rho=1}^{1000} \breve{\xi}^{(\rho)},$$

respectively, where $\breve{\xi}^{(\rho)}$ is the offered estimate of ξ at ith simulated sample.

For each combination of full sample size n, inspection points τ_i, stress points δ_i, and progressive proportions π_i for $i = 1, 2, 3, 4$, we evaluate all analytical results of ξ (as an example) based on the following criteria:

a. Mean Absolute Bias (MAB):

$$\text{MAB}(\breve{\xi}) = \frac{1}{1000}\sum_{\rho=1}^{1000}\left|\breve{\xi}^{(\rho)} - \xi\right|,$$

b. Root Mean Squared-Error (RMSE):

$$\text{RMSE}(\breve{\xi}) = \sqrt{\frac{1}{1000}\sum_{\rho=1}^{1000}\left(\breve{\xi}^{(\rho)} - \xi\right)^2},$$

c. Average Interval Length (AIL):

$$\text{AIL}_{\xi}^{(1-\varnothing)\%} = \frac{1}{1000}\sum_{\rho=1}^{1000}\left(\mathcal{U}_{\breve{\xi}^{(\rho)}} - \mathcal{L}_{\breve{\xi}^{(\rho)}}\right),$$

and

d. Coverage Percentage (CP):

$$\text{CP}_{\xi}^{(1-\varnothing)\%} = \frac{1}{1000}\sum_{\rho=1}^{1000}\boldsymbol{D}^{\diamond}_{\left(\mathcal{L}_{\breve{\xi}^{(\rho)}};\mathcal{U}_{\breve{\xi}^{(\rho)}}\right)}(\xi),$$

respectively, where $\boldsymbol{D}^{\diamond}(\cdot)$ denotes the indicator, and $(\mathcal{L}(\cdot), \mathcal{U}(\cdot))$ denotes the interval limits of ξ.

Besides the proposed numerical investigations on the unknown parameters ξ and δ_i, $i = 1, 2, 3, 4$, according to variance and optimality criteria, we also determine the optimal lengths of inspection intervals, say $\tau_V^{\star}$ and $\tau_D^{\star}$, respectively. The estimation outputs of θ, δ_1, δ_2, and δ_3 are reported in Tables 1–4. Tables 5–6 list the fitted values for the optimal criteria $\tau_V^{\star}$ and $\tau_D^{\star}$.

Table 1: Estimates of ξ in Monte Carlo simulation

PC	n	MLE			ACI		Boot	
		Av. E	AB	RMSE	AIL	CP	AIL	CP
				Stress-I				
PC [1]	30	1.173	0.673	0.703	0.832	0.928	1.475	0.906
	60	1.146	0.646	0.662	0.564	0.934	0.891	0.925
	100	1.141	0.641	0.650	0.427	0.937	0.615	0.931
	150	1.138	0.638	0.645	0.346	0.941	0.483	0.936
	200	1.137	0.637	0.642	0.299	0.944	0.457	0.938

(Continued)

Table 1 (continued)

PC	n	MLE			ACI		Boot	
		Av. E	AB	RMSE	AIL	CP	AIL	CP
PC [2]	30	1.095	0.601	0.644	0.745	0.930	0.964	0.921
	60	1.072	0.572	0.598	0.516	0.936	0.720	0.928
	100	1.065	0.565	0.581	0.397	0.939	0.538	0.935
	150	1.061	0.561	0.571	0.323	0.942	0.428	0.938
	200	1.058	0.558	0.566	0.280	0.945	0.377	0.941
PC [3]	30	1.047	0.570	0.622	0.728	0.932	0.766	0.930
	60	1.020	0.523	0.561	0.503	0.937	0.580	0.935
	100	1.000	0.500	0.524	0.387	0.940	0.430	0.938
	150	0.989	0.489	0.506	0.316	0.943	0.354	0.941
	200	0.988	0.488	0.503	0.274	0.946	0.308	0.943
				Stress-II				
PC [1]	30	1.071	0.573	0.601	0.727	0.932	1.312	0.909
	60	1.056	0.556	0.571	0.500	0.937	0.681	0.928
	100	1.053	0.553	0.562	0.385	0.941	0.596	0.934
	150	1.052	0.552	0.558	0.308	0.945	0.481	0.939
	200	1.051	0.551	0.555	0.263	0.948	0.422	0.941
PC [2]	30	1.027	0.536	0.570	0.679	0.934	0.771	0.924
	60	1.007	0.507	0.530	0.473	0.940	0.588	0.931
	100	0.996	0.496	0.511	0.363	0.943	0.469	0.938
	150	0.990	0.490	0.501	0.295	0.946	0.418	0.941
	200	0.988	0.488	0.497	0.255	0.949	0.344	0.944
PC [3]	30	0.965	0.497	0.538	0.657	0.936	0.723	0.933
	60	0.948	0.457	0.487	0.460	0.941	0.516	0.938
	100	0.940	0.442	0.467	0.356	0.944	0.388	0.941
	150	0.923	0.424	0.442	0.290	0.947	0.332	0.944
	200	0.911	0.411	0.427	0.251	0.949	0.280	0.946

Table 2: Estimates of δ_1 in Monte Carlo simulation

PC	n	MLE			ACI		Boot	
		Av. E	MAB	RMSE	AIL	CP	AIL	CP
				Stress-I				
PC [1]	30	1.319	0.843	0.977	2.089	0.875	2.855	0.864
	60	1.284	0.787	0.870	1.431	0.904	1.755	0.898
	100	1.271	0.771	0.826	1.090	0.912	1.402	0.901

(Continued)

Table 2 (continued)

PC	n	MLE			ACI		Boot	
		Av. E	MAB	RMSE	AIL	CP	AIL	CP
	150	1.267	0.767	0.806	0.879	0.915	1.245	0.906
	200	1.267	0.767	0.796	0.768	0.918	1.158	0.909
PC [2]	30	1.163	0.749	0.879	1.829	0.883	2.192	0.875
	60	1.139	0.658	0.763	1.253	0.907	1.685	0.902
	100	1.122	0.625	0.704	0.970	0.914	1.290	0.905
	150	1.113	0.615	0.672	0.792	0.918	1.069	0.910
	200	1.110	0.610	0.654	0.686	0.923	0.967	0.912
PC [3]	30	1.101	0.735	0.889	1.799	0.885	2.090	0.878
	60	1.065	0.618	0.728	1.236	0.908	1.492	0.904
	100	1.036	0.560	0.657	0.941	0.916	1.136	0.906
	150	1.012	0.526	0.612	0.764	0.920	0.963	0.912
	200	1.021	0.528	0.612	0.660	0.924	0.847	0.916
				Stress-II				
PC [1]	30	1.133	0.653	0.743	1.557	0.890	2.615	0.879
	60	1.122	0.625	0.684	1.064	0.919	1.414	0.913
	100	1.112	0.612	0.653	0.813	0.928	1.110	0.918
	150	1.106	0.606	0.636	0.649	0.931	0.968	0.921
	200	1.106	0.606	0.627	0.553	0.936	0.887	0.924
PC [2]	30	1.050	0.609	0.721	1.392	0.898	1.789	0.890
	60	1.025	0.542	0.619	0.947	0.922	1.292	0.917
	100	0.997	0.503	0.565	0.726	0.930	1.087	0.920
	150	0.983	0.485	0.534	0.592	0.934	0.900	0.924
	200	0.981	0.482	0.520	0.514	0.938	0.809	0.928
PC [3]	30	0.926	0.579	0.693	1.337	0.900	1.572	0.893
	60	0.905	0.472	0.559	0.940	0.923	1.133	0.919
	100	0.890	0.426	0.498	0.719	0.932	0.922	0.921
	150	0.860	0.387	0.452	0.583	0.936	0.760	0.928
	200	0.840	0.357	0.421	0.505	0.939	0.655	0.932

Table 3: Estimates of δ_2 in Monte Carlo simulation

PC	n	MLE			ACI		Boot	
		Av.E	MAB	RMSE	AIL	CP	AIL	CP
				Stress-I				
PC [1]	30	1.593	0.613	0.711	1.716	0.907	2.347	0.893
	60	1.105	0.465	0.586	1.218	0.913	1.648	0.906
	100	1.029	0.376	0.470	0.948	0.916	1.298	0.911
	150	0.986	0.312	0.393	0.776	0.920	1.090	0.914
	200	0.979	0.287	0.340	0.697	0.922	0.969	0.916
PC [2]	30	1.208	0.655	0.855	1.855	0.904	2.633	0.884
	60	0.565	0.576	0.746	1.262	0.911	1.727	0.902
	100	0.499	0.561	0.685	0.963	0.915	1.353	0.907
	150	1.560	0.570	0.648	0.782	0.919	1.184	0.912
	200	1.557	0.561	0.622	0.676	0.920	1.120	0.914
PC [3]	30	0.310	0.879	0.968	2.618	0.890	3.218	0.876
	60	0.200	0.813	0.914	1.539	0.904	1.884	0.897
	100	0.134	0.867	0.936	1.176	0.913	1.518	0.903
	150	0.084	0.916	0.967	0.956	0.915	1.228	0.908
	200	0.082	0.918	0.965	0.839	0.917	1.142	0.912
				Stress-II				
PC [1]	30	1.347	0.568	0.700	1.857	0.903	2.557	0.889
	60	1.275	0.404	0.501	1.321	0.909	1.934	0.898
	100	1.263	0.347	0.427	1.027	0.912	1.523	0.903
	150	1.238	0.298	0.364	0.842	0.916	1.263	0.907
	200	1.233	0.278	0.336	0.733	0.918	1.117	0.912
PC [2]	30	0.748	0.575	0.714	2.068	0.901	3.143	0.882
	60	0.669	0.471	0.579	1.397	0.907	2.315	0.893
	100	0.630	0.442	0.533	1.072	0.912	1.776	0.900
	150	0.605	0.428	0.506	0.871	0.915	1.468	0.904
	200	0.596	0.425	0.491	0.756	0.916	1.358	0.906
PC [3]	30	1.748	0.832	1.005	2.789	0.887	4.532	0.871
	60	1.646	0.688	0.810	1.624	0.900	2.387	0.891
	100	0.565	0.576	0.746	1.249	0.911	1.831	0.897
	150	0.429	0.589	0.694	0.989	0.912	1.546	0.902
	200	0.387	0.621	0.710	0.843	0.916	1.370	0.904

Table 4: Estimates of δ_3 in Monte Carlo simulation

PC	n	MLE			ACI		Boot	
		Av. E	MAB	RMSE	AIL	CP	AIL	CP
				Stress-I				
PC [1]	30	1.816	0.568	0.714	1.648	0.897	1.850	0.894
	60	1.749	0.419	0.519	1.211	0.912	1.360	0.909
	100	1.700	0.336	0.417	0.954	0.916	1.072	0.914
	150	1.673	0.284	0.353	0.789	0.921	0.886	0.916
	200	1.673	0.256	0.319	0.687	0.925	0.771	0.919
PC [2]	30	1.061	0.698	0.891	1.954	0.900	2.174	0.887
	60	1.004	0.611	0.743	1.525	0.907	1.586	0.903
	100	0.966	0.582	0.687	1.124	0.912	1.251	0.909
	150	0.938	0.577	0.663	0.926	0.916	1.031	0.912
	200	0.930	0.575	0.648	0.806	0.919	0.897	0.915
PC [3]	30	0.640	1.008	1.274	2.331	0.883	2.501	0.879
	60	0.566	1.040	1.133	1.623	0.902	1.742	0.898
	100	0.508	1.031	1.109	1.272	0.910	1.365	0.907
	150	0.460	0.998	1.126	1.043	0.914	1.120	0.911
	200	0.469	0.972	1.106	0.907	0.916	0.973	0.912
				Stress-II				
PC [1]	30	1.549	0.471	0.579	1.741	0.894	1.993	0.890
	60	1.485	0.345	0.434	1.230	0.911	1.409	0.907
	100	1.473	0.270	0.338	0.981	0.913	1.123	0.910
	150	1.449	0.220	0.278	0.814	0.919	0.932	0.913
	200	1.445	0.194	0.245	0.710	0.923	0.813	0.915
PC [2]	30	1.398	0.670	0.892	2.070	0.888	2.349	0.883
	60	1.318	0.494	0.619	1.459	0.904	1.655	0.900
	100	1.249	0.442	0.553	1.159	0.910	1.316	0.903
	150	1.207	0.404	0.508	0.959	0.914	1.088	0.911
	200	1.204	0.379	0.470	0.837	0.916	0.949	0.913
PC [3]	30	0.904	0.917	1.272	2.525	0.879	2.763	0.876
	60	0.853	0.775	0.996	1.695	0.900	1.855	0.896
	100	0.806	0.743	0.907	1.333	0.907	1.459	0.905
	150	0.726	0.792	0.917	1.096	0.912	1.199	0.911
	200	0.684	0.823	0.929	0.954	0.914	1.044	0.910

Table 5: Optimum inspection times $\tau_V^\star$ and $\tau_D^\star$ in Monte Carlo simulation at Stress-I

PC	n	$k=2$		$k=3$		$k=4$	
		$\tau_V^\star$	$\tau_D^\star$	$\tau_V^\star$	$\tau_D^\star$	$\tau_V^\star$	$\tau_D^\star$
PC [1]	30	0.7897	0.3818	0.3505	0.0747	0.0508	0.0142
	60	0.3939	0.3545	0.1751	0.0673	0.0254	0.0124
	100	0.2353	0.3319	0.1051	0.0587	0.0152	0.0103
	150	0.1550	0.3235	0.0696	0.0559	0.0101	0.0094
	200	0.1151	0.3190	0.0522	0.0545	0.0076	0.0091
PC [2]	30	0.8749	0.7794	0.3764	0.1751	0.0558	0.0290
	60	0.4360	0.7133	0.1832	0.1729	0.0274	0.0263
	100	0.2615	0.6857	0.1099	0.1298	0.0163	0.0173
	150	0.1727	0.6386	0.0726	0.1153	0.0108	0.0146
	200	0.1288	0.6222	0.0543	0.1099	0.0080	0.0137
PC [3]	30	1.0399	72.988	0.4685	15.024	0.0710	9.4136
	60	0.5197	9.1610	0.2311	4.8917	0.0351	3.5934
	100	0.3110	1.3062	0.1385	0.2614	0.0206	0.0269
	150	0.2073	1.1369	0.0913	0.2282	0.0135	0.0243
	200	0.1540	0.9657	0.0678	0.2072	0.0101	0.0242

Table 6: Optimum inspection times $\tau_V^\star$ and $\tau_D^\star$ in Monte Carlo simulation at Stress-II

PC	n	$k=2$		$k=3$		$k=4$	
		$\tau_V^\star$	$\tau_D^\star$	$\tau_V^\star$	$\tau_D^\star$	$\tau_V^\star$	$\tau_D^\star$
PC [1]	30	0.7066	3.4859	0.2496	2.5627	0.0421	1.3039
	60	0.3513	0.8747	0.1239	0.1246	0.0205	0.0244
	100	0.2102	0.8379	0.0743	0.1147	0.0122	0.0207
	150	0.1396	0.8173	0.0494	0.1090	0.0081	0.0190
	200	0.1045	0.8030	0.0370	0.1051	0.0061	0.0180
PC [2]	30	0.8591	230.21	0.2909	55.895	0.0475	23.689
	60	0.4035	1.6497	0.1368	0.2212	0.0224	0.0341
	100	0.2416	1.5785	0.0804	0.2172	0.0131	0.0327
	150	0.1608	1.5732	0.0532	0.1974	0.0086	0.0273
	200	0.1202	1.5208	0.0398	0.1839	0.0064	0.0248
PC [3]	30	0.9318	360.94	0.4203	124.75	0.0608	59.221
	60	0.4932	58.234	0.1681	35.771	0.0273	24.344
	100	0.2934	20.429	0.0990	14.281	0.0161	11.436
	150	0.1885	19.309	0.0636	6.9202	0.0102	5.8705
	200	0.1394	4.3404	0.0467	0.5042	0.0074	0.0621

From Tables 1–4, regarding the efficient estimation that provides the lowest MABs, RMSEs, and AILs, as well as the highest CPs, we reach the following conclusions:

- All offered estimates of ξ and $\delta_i,\ i = 1,2,3$, serve good performance; that is the main observation point.
- As n tends to grow, all point (or interval) results of ξ and $\delta_i,\ i = 1,2,3$, perform satisfactorily.
- As $\delta_i,\ i = 1,2,3$, increase, it can be seen that:
  - The MABs and RMSEs of ξ and $\delta_i,\ i = 1,2,3$, decreased.
  - The AILs of ξ and δ_1 decreased while those of $\delta_i,\ i = 2,3$, increased. The opposite performance is observed in the comparison case based on their CP values.
- As $\pi_i,\ i = 2,3,4$, increase (when $\pi_4 = 1$), the simulated MAB, RMSE, and AIL values of ξ and δ_1 decreased while the associated CP values increased. The opposite observation is observed for the estimation of δ_2 and δ_3.
- Comparing the interval estimates provided for ξ and $\delta_i,\ i = 1,2,3,$, it is observed that the proposed asymptotic interval approach behaves superiorly compared to the bootstrapping interval approach.
- In most scenarios, the CP values for all asymptotic (or bootstrapped) interval estimates exceed the nominal 95% significance level.
- Lastly, we can sum up that both likelihood and asymptotic estimation methodologies behave well in turn to estimate the LBE parameter in the presence of a data set available from PIC-T1 using the k-stage step-stress P-ALT.

From Tables 5–6, regarding the estimated criteria of an optimal time inspection, we provide the following comments:

- When n increases, the estimates of $\tau_V^\star$ and $\tau_D^\star$ narrowed down. Thus, the greater the number of test units (n), the longer the ideal inspection duration.
- When k increases, the estimates of $\tau_V^\star$ and $\tau_D^\star$ narrowed down. That is, the higher the stress level, the shorter the examination period.
- When $\pi_i,\ i = 2,3,4$, increase (when $\pi_4 = 1$), the estimates of $\tau_V^\star$ and $\tau_D^\star$ increased. This fact means that the greater the number of subjects to be excluded at each stage, the shorter the optimal period for inspection.
- If one aims to stop the test more quickly, the level of $\pi_i,\ i = 2,3,4$, should rise.
- When $\delta_i,\ i = 1,2,3$, grew, the estimates of $\tau_V^\star$ decreased while those of $\tau_D^\star$ increased.

7 Hardened-Steel Data Analysis

To highlight the adaptability of the proposed methods to practice, a physics data set consisting of ordered times to failure in rolling contact fatigue of ten hardened steel specimens is analyzed. These times were tested at each of four values of contact stress and recorded using a 4-ball rolling contact tester at Mobil Research and Development's Princeton laboratories; see Yan et al. [19]. In Table 7, four groups of hardened steel failure times, each consisting of ten observations, are reported. Before going to draw the proposed estimations, to check if the LBE lifetime distribution is a suitable model to fit the hardened steel data sets or not, for each group, the Kolmogorov–Smirnov (KS) statistic (with its$P$-value) is obtained; see Table 8. Additionally, the MLE (with its standard error (Std.Err)) of ξ at each stress level is also developed in Table 8. It indicates that the LBE distribution fits the hardened steel data set so well.

Table 7: Four groups of hardened steel failure times

Stress	Times									
0.87 (10^6psi)	1.67	2.20	2.51	3.00	3.90	4.70	7.53	14.70	27.8	37.4
0.99 (10^6psi)	0.80	1.00	1.37	2.25	2.95	3.70	6.07	6.65	7.05	7.37
1.09 (10^6psi)	0.012	0.18	0.20	0.24	0.26	0.32	0.32	0.42	0.44	0.88
1.18 (10^6psi)	0.073	0.098	0.117	0.135	0.175	0.262	0.270	0.350	0.386	0.456

Table 8: The MLE and KS from hardened steel data

Stress	MLE		KS	
	Est.	Std. Err	Distance	*P*-value
0.87 (10^6psi)	5.2705	1.1785	0.3755	0.0895
0.99 (10^6psi)	1.9605	0.4384	0.2148	0.6708
1.09 (10^6psi)	0.1636	0.0365	0.2011	0.8135
1.18 (10^6psi)	0.1161	0.0259	0.1591	0.9289

Several comprehensive data visualizations have been meticulously constructed to offer an in-depth understanding of the model's behavior and the adequacy of its fit to the observed data. These graphical tools include the estimated/empirical RF and estimated/empirical PDF overlaid with histograms specifically derived from hardened steel lifetime data, as well as diagnostic plots such as the probability-probability (P-P) and quantile-quantile (Q-Q) plots. Collectively, these visualizations serve to validate the proposed model, assess its fit, and highlight potential deviations between theoretical and empirical distributions under various stress levels; see Fig. 2. Fig. 2a,b demonstrates good alignment between the estimated LBE model and the empirical reliability and probability density functions, with the PDF overlaying a histogram of hardened steel lifetimes. Fig. 2c,d shows points close to the theoretical lines, indicating that the model provides a reasonably good fit to the observed hardened steel data. To show the existence and uniqueness of the MLE $\hat{\xi}$, at each stress level, Fig. 3 indicates that all fitted values of $\hat{\xi}$ (reported in Table 8) existed and are unique. To distinguish, in Fig. 3, the red line represents the log-likelihood as a function of ξ, while the blue line marks its maximum log-likelihood value.

Now, to examine the acquired theoretical results, several samples are obtained from the fully hardened steel data set under step-stress P-ALT via PIC-T1. Following Sief et al. [20], in Table 9, various PIC-T1 data sets are simulated randomly and reported. These samples are collected based on different options of τ_i, $i = 1, \dots, 5$, (inspection periods) and τ_i, $i = 1, \dots, 5$, (proportion styles of PC) when the stress levels are assigned as $\delta_1 = 0.87(10^6\text{psi})$, $\delta_2 = 0.99(10^6\text{psi})$, $\delta_3 = 1.09(10^6\text{psi})$, and $\delta_4 = 1.18(10^6\text{psi})$; see Table 9.

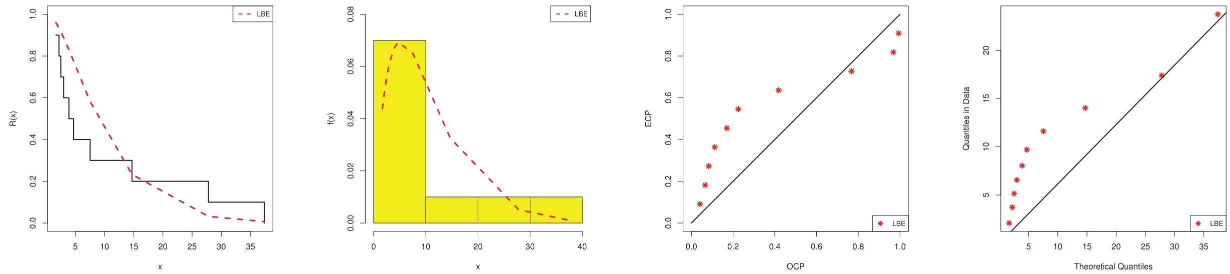

(i) $0.87(10^6\text{psi})$

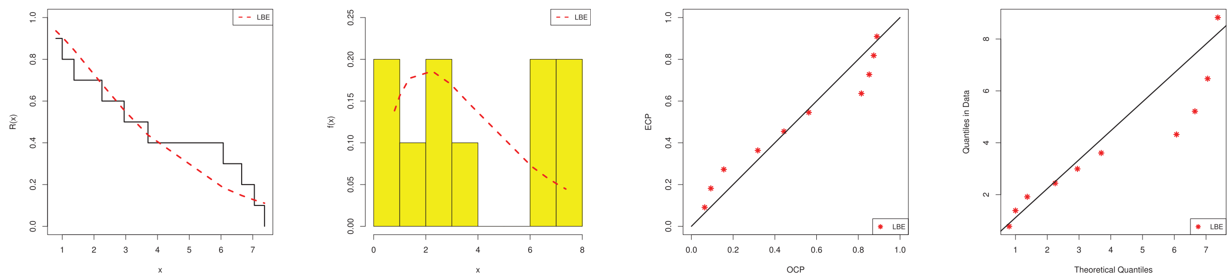

(ii) $0.99(10^6\text{psi})$

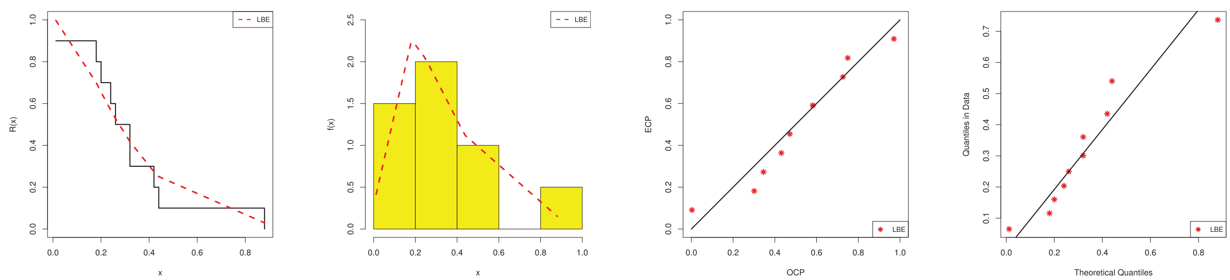

(iii) $1.09(10^6\text{psi})$

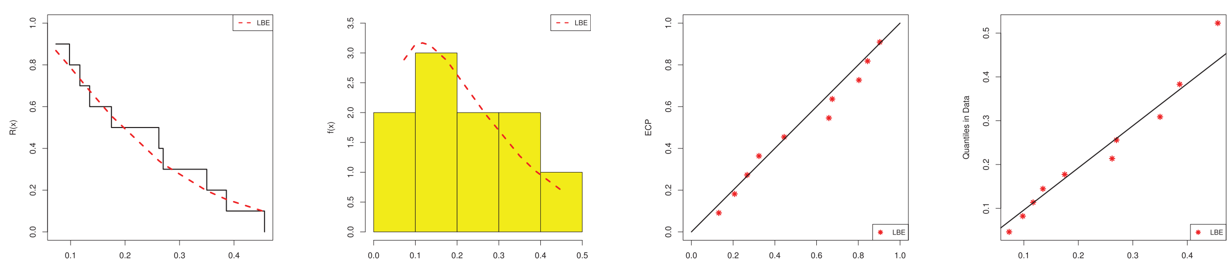

(iv) $1.18(10^6\text{psi})$

(a) Reliability (b) Density (c) P-P (d) Q-Q

Figure 2: Four data visualizations from hardened steel data

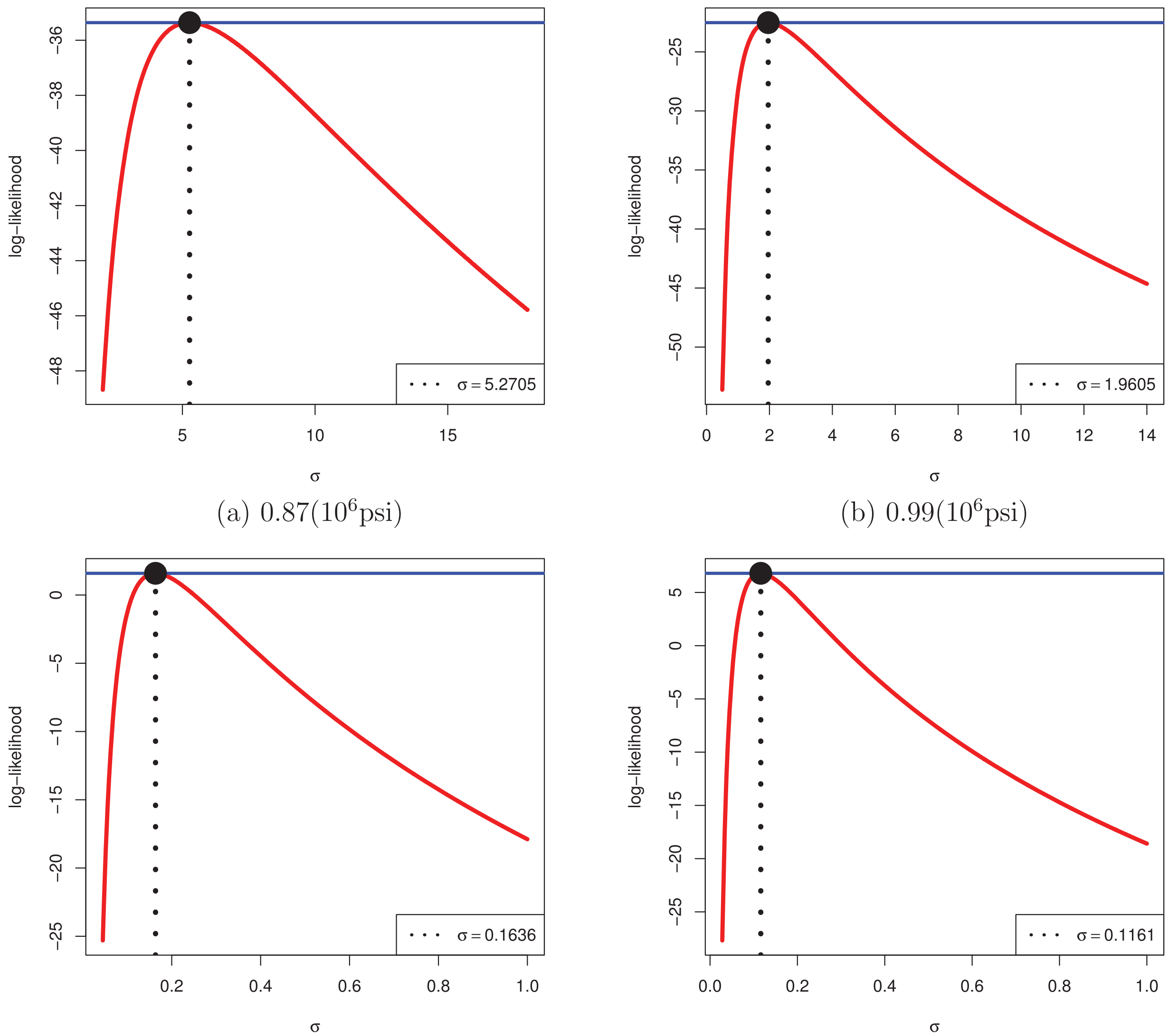

(a) $0.87(10^6\text{psi})$ (b) $0.99(10^6\text{psi})$

(c) $1.09(10^6\text{psi})$ (d) $1.18(10^6\text{psi})$

Figure 3: Four log-likelihoods of ξ from hardened steel data

We now assess the performance of the point estimations (with their Std. Errs) and interval estimations (with their interval-widths (IWs)) of ξ and δ_i, $i = 1, 2, 3, 4$; see Table 10. It indicates that the acquired estimates of all unknown subjects perform adequately in terms of their Std. Err and IW values. It is also clear that the IWs obtained via the ACI approach behave well compared to those obtained via the bootstrap approach. Furthermore, Fig. 4 shows that all estimates of ξ and δ_i, $i = 1, 2, 3, 4$, existed and are unique.

Moreover, from Table 9, to assess the optimal lengths of inspection intervals, we fitted the variance and optimality criteria; see Table 11. It shows that the results of $\tau_V^\star$ and $\tau_D^\star$ increased when the PC's proportions increased. The opposite fact was also recorded when the inspection levels increased.

Table 9: Different PIC-T1 samples from hardened steel data

PC	Stress level	$(\tau_1, \tau_2, \tau_3, \tau_4, \tau_5)$	$(\pi_1, \pi_2, \pi_3, \pi_4, \pi_5)$	$(n_1, n_2, n_3, n_4, n_5)$	$(m_1, m_2, m_3, m_4, m_5)$
PC [A]	δ_1	(0.1, 0.5, 1, 1.5, 2)	(0.05, 0.05, 0.05, 0.05, 1)	(0,0,0,0,1)	(0,0,0,0,9)
	δ_2			(0,0,2,1,0)	(0,0,0,0,7)
	δ_3			(1,8,1,0,0)	(0,0,0,0,0)
	δ_4			(2,8,0,0,0)	(0,0,0,0,0)
PC [B]	δ_1	(0.3, 0.8, 1.3, 1.8, 2.3)	(0.15, 0.15, 0.15, 0.15, 1)	(0,0,0,1,1)	(1,1,1,0,5)
	δ_2			(0,1,1,1,1)	(1,1,0,0,4)
	δ_3			(5,4,1,0,0)	(0,0,0,0,0)
	δ_4			(7,3,0,0,0)	(0,0,0,0,0)
PC [C]	δ_1	(0.4, 1, 1.5, 2, 2.5)	(0.25, 0.25, 0.25, 0.25, 1)	(0,0,0,1,1)	(2,2,1,1,2)
	δ_2			(0,2,1,0,1)	(2,1,1,0,2)
	δ_3			(7,3,0,0,0)	(0,0,0,0,0)
	δ_4			(9,1,0,0,0)	(0,0,0,0,0)

Table 10: Estimates of ξ and $\delta_i,\ i = 1, 2, 3, 4$, from hardened steel data set

Par.	MLE		95% ACI			95% Boot		
	Estimate	Std. Err	Lower	Upper	IW	Lower	Upper	IW
				PC [A]				
ξ	0.2503	0.0166	0.2179	0.2828	0.0649	0.1852	0.3876	0.2024
δ_1	0.4597	0.0576	0.3467	0.5726	0.2259	0.3047	0.6329	0.3282
δ_2	0.3946	0.0555	0.0257	0.5034	0.4777	0.0169	0.5403	0.5234
δ_3	0.9745	0.0243	0.9343	1.0294	0.0951	0.8775	1.0987	0.2212
δ_4	1.1907	0.0074	1.1746	1.2036	0.0290	1.1125	1.2710	0.1585
				PC [B]				
ξ	0.4058	0.0192	0.3683	0.4434	0.0751	0.3317	0.4991	0.1674
δ_1	0.2907	0.0169	0.1770	0.3837	0.2067	0.1546	0.3795	0.2249
δ_2	0.3221	0.0438	0.2651	0.4369	0.1718	0.2564	0.5678	0.3114
δ_3	0.7025	0.0220	0.6635	0.7499	0.0864	0.6461	0.8257	0.1796
δ_4	1.1592	0.0063	1.1190	1.1823	0.0633	1.0018	1.1296	0.1278
				PC [C]				
ξ	0.3976	0.0188	0.3607	0.4345	0.0738	0.3114	0.4380	0.1266
δ_1	0.1327	0.0248	0.0841	0.1813	0.0972	0.0752	0.2188	0.1436
δ_2	0.5204	0.0281	0.4649	0.5751	0.1101	0.4118	0.5642	0.1524
δ_3	0.7411	0.0026	0.7349	0.7451	0.0102	0.6798	0.7970	0.1172
δ_4	1.1654	0.0017	1.1597	1.1663	0.0067	1.0987	1.1969	0.0982

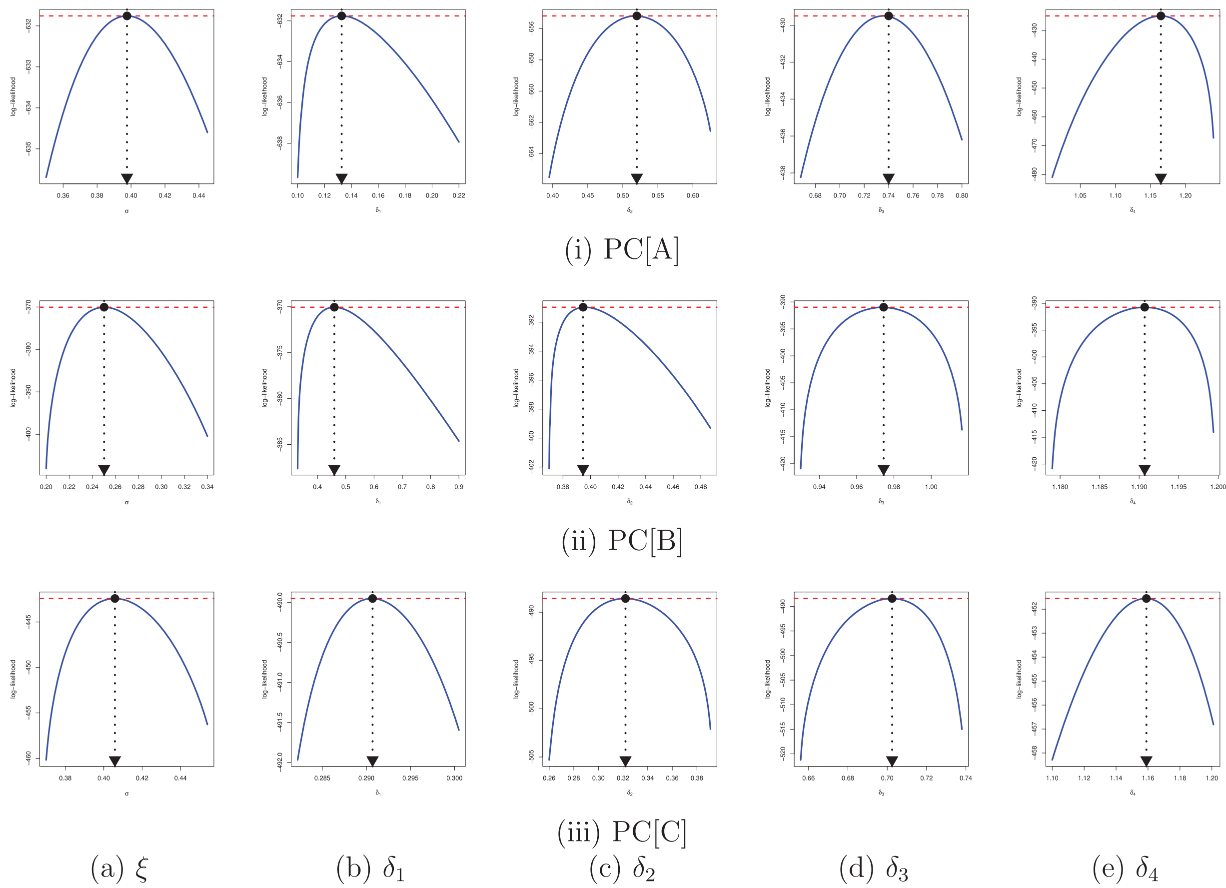

Figure 4: The log-likelihoods of ξ and δ_i, $i = 1, 2, 3, 4$, from hardened steel data

Table 11: Optimum inspection times $\tau_V^\star$ (1st Col.) and $\tau_D^\star$ (2nd Col.) from hardened steel data set

PC	$k = 2$		$k = 3$		$k = 4$		$k = 5$	
PC [A]	0.00313	254.175	0.00283	198.743	0.00187	169.741	0.00105	127.822
PC [B]	0.00451	316.795	0.00447	278.432	0.00279	255.983	0.00184	186.036
PC [C]	0.01011	449.463	0.00965	419.984	0.00949	364.129	0.00927	287.427

8 Conclusions

In this study, we examined the use of progressive censoring, step-stress P-ALT, and interval data to create step-stress P-ALTs with PIC-T1 data. The LBE lifetime distribution at each stress level was examined. Determining the optimum length of the inspection interval is a significant issue for experimenters when analyzing the reliability of increasingly interval-censored life test data for particular stress levels and test unit counts. The proposed asymptotic interval strategy performs better than the bootstrapping interval approach. Two optimality criteria (var-optimality and D-optimality) for determining the optimal length of the inspection interval were utilized for comparison. Certain life tests necessitate the removal of test units at points other than the experiment's final termination point;

therefore, screening the test units continuously is impractical. The PIC-T1 system allows units to be eliminated early and reviewed periodically. The results provide useful information to practitioners in setting up appropriate life test plans under increasing Type-I interval censoring.

Acknowledgement: The authors would like to express thank to the Editor-in-Chief and anonymous referees for their constructive comments and suggestions. The authors express their gratitude to Princess Nourah bint Abdulrahman University Researchers Supporting Project number (PNURSP2025R50), Princess Nourah bint Abdulrahman University, Riyadh, Saudi Arabia.

Funding Statement: This research was funded by the Princess Nourah bint Abdulrahman University Researchers Supporting Project number (PNURSP2025R50), Princess Nourah bint Abdulrahman University, Riyadh, Saudi Arabia.

Author Contributions: The authors confirm contribution to the paper as follows: study conception and design: Refah Alotaibi, Hoda Rezk, Ahmed Elshahhat; data collection: Refah Alotaibi; analysis and interpretation of results: Chanseok Park, Hoda Rezk, Ahmed Elshahhat; draft manuscript preparation: Refah Alotaibi. Ahmed Elshahhat. All authors reviewed the results and approved the final version of the manuscript.

Availability of Data and Materials: The data that support the findings of this study are available within the paper.

Ethics Approval: Not applicable.

Conflicts of Interest: The authors declare no conflicts of interest to report regarding the present study.

References

1. Ismail AA. Optimum partially accelerated life test plans with progressively Type I interval-censored data. Seq Anal. 2015;34(2):135–47. doi:10.1080/07474946.2015.1030301.
2. Nelson W. Accelerated life testing: statistical models, data analysis and test plans. New York, NY, USA: John Wiley and Sons; 1990.
3. Tang LC, Sun YS, Goh TN, Ong HL. Analysis of step-stress accelerated-life–test data: a new approach. IEEE Trans Reliability. 1996;45(1):69–74. doi:10.1109/24.488919.
4. Xiong C. Inferences on a simple step-stress model with type-II censored exponential data. IEEE Trans Reliability. 1998;47(2):142–6. doi:10.1109/24.722278.
5. Gouno E, Sen A, Balakrishnan N. Optimal step stress test under progressive type-I censoring. IEEE Trans Reliability. 2004;53(3):388–93. doi:10.1109/tr.2004.833320.
6. Abdel-Hamid AH, Al-Hussaini E. Estimation in step-stress accelerated life tests for the exponentiated exponential distribution with type I censoring. Comput Statist Data Anal. 2009;53(4):1328–38. doi:10.1016/j.csda.2008.11.006.
7. Ismail AA, Aly HM. Optimal planning of failure-step stress partially accelerated life tests under type-II censoring. Statist Comput Simul. 2010;80(12):1335–48. doi:10.1080/00949650903071096.
8. Pushkarna N, Saran J, Nain J, Verma K. Progressively Type-II right censored order statistics from Hjorth distribution and related inference. Stat Optim Inf Comput. 2020;8(2):481–98. doi:10.19139/soic-2310-5070-751.

9. EL-Sagheer RM, Hasaballah MM. Inference of process capability index Cpy for 3-Burr–XII distribution based on progressive Type-II censoring. Inter J Math Mathal Sci. 2020;2020(3):1–13. doi:10.1155/2020/2412857.
10. Alotaibi R, Almetwally EM, Hai Q, Rezk H. Optimal test plan of step stress partially accelerated life testing for alpha power inverse Weibull distribution under adaptive progressive hybrid censored data and different loss functions. Mathematics. 2022;10(24):4652. doi:10.3390/math10244652.
11. Prakash A, Maurya RK, Alsadat N, Obulezi OJ. Parameter estimation for reduced Type-I Heavy-Tailed Weibull distribution under progressive Type-II censoring scheme. Alex Eng J. 2024;109:935–49. doi:10.1016/j.aej.2024.09.029.
12. Maurya RK, Tripathi YM, Sen T, Rastogi MK. On progressively censored inverted exponentiated Rayleigh distribution. J Stat Comput Simul. 2019;89(3):492–518. doi:10.1080/00949655.2018.1558225.
13. Rahman A, Kamal M, Khan S, Khan MF, Mustafa MS, Hussam E, et al. Statistical inferences under step stress partially accelerated life testing based on multiple censoring approaches using simulated and real-life engineering data. Sci Rep. 2023;13(1):12452. doi:10.1038/s41598-023-39170-x.
14. Newer HA, Abd-El–Monem A, Al-Shbeil I, Emam W, Nower M. Optimal test plans for accelerated life tests based on progressive type-I censoring with engineering applications. Alex Eng J. 2024;87(2):604–21. doi:10.1016/j.aej.2023.12.038.
15. Dara ST, Ahmad M. Recent advances in moment distribution and their hazard rates. Saarbrücken, Germany: Lap Lambert Academic Publishing GmbH KG; 2012.
16. Deshmukh S, Kulkarni M. Introduction. In: Asymptotic statistical inference. Singapore: Springer; 2021.
17. Chernick MR, LaBudde RA. An introduction to bootstrap methods with applications to R. New York, NY, USA: John Wiley and Sons; 2014.
18. Bai DS, Kim JG, Chun YR. Design of failure censored accelerated life test sampling plans for lognormal and Weibull distributions. Eng Optim. 1993;21(3):197– 212. doi:10.1080/03052159308940975.
19. Yan Z, Zhu T, Peng X, Li X. Reliability analysis for multi-level stress testing with Weibull regression model under the general progressively Type-II censored data. J Comput Appl Math. 2018;330(3):28–40. doi:10.1016/j.cam.2017.05.048.
20. Sief M, Liu X, Abd El-Raheem AERM. Inference for a constant-stress model under progressive type-I interval censored data from the generalized half-normal distribution. J Stat Comput Simul. 2021;91(15):3228–53. doi:10.1080/00949655.2021.1925673.